Journal of Molecular Structure 1034 (2013) 62–68

Contents lists available at SciVerse ScienceDirect

Journal of Molecular Structure

journal homepage: www.elsevier.com/locate/molstruc

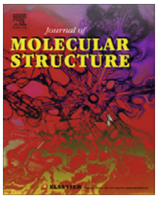

Functionalization of the benzobicyclo[3.2.1]octadiene skeleton via photocatalytic oxygenation of furan and benzofuran derivatives

Ilijana Kikaš [a], Ottó Horváth [b,*], Irena Škorić [a,*]

[a] *Department of Organic Chemistry, Faculty of Chemical Engineering and Technology, University of Zagreb, Marulićev trg 19, 10000 Zagreb, Croatia*

[b] *Department of General and Inorganic Chemistry, Institute of Chemistry, Faculty of Engineering, University of Pannonia, P.O.B. 158, Veszprém H-8201, Hungary*

HIGHLIGHTS

- ▶ Free-base and manganese(III) porphyrins as efficient photocatalysts of oxygenation.
- ▶ Catalyst-depending products of a furan derivative of benzobicyclo[3.2.1]octadiene.
- ▶ Deviating mechanisms of oxygenation, simultaneous electronic and steric effects.
- ▶ An additional, shielding benzene ring hinders formation of different products.

ARTICLE INFO

Article history:
Received 28 May 2012
Received in revised form 12 August 2012
Accepted 3 September 2012
Available online 11 September 2012

Keywords:
Photocatalytic oxygenation
Porphyrins
Benzobicyclo[3.2.1]octadienes
(Benzo)furan derivative
10-Membered keto-lactone derivative

ABSTRACT

Photocatalytic oxygenations of a furan and a benzofuran derivative have been realized by using anionic and cationic free-base porphyrins as well as their manganese(III) complexes under various reaction conditions. In the case of the furan derivative, application of these catalysts resulted in deviating reaction pathways generating different products. Annulation of a benzene to the outer side of the furan ring, however, led to the formation of only one type of product, independently of the photocatalyst used. Different oxygenation mechanisms leading to the same end-product, the 10-membered keto-lactone derivative, have been suggested for the metalloporphyrins and the corresponding free bases.

1. Introduction

Photocatalytic processes proved to be successful in both natural and artificial systems such as photosynthesis, the basis of the food chain on Earth [1], and oxidative degradation of various harmful organic pollutants, e.g. polyaromatic hydrocarbon (PAH) derivatives [2] and surfactants [3]. Connecting to the latter area, in photodynamic therapy (PDT) also oxidation of organic compounds, moreover, living organisms can be performed by application of various sensitizers such as porphyrins, the excitation of which leads to in situ generation of singlet oxygen, a very oxidative species, in the tissue of malignant tumors [4]. However, singlet oxygen can also be utilized for preparative purposes, for synthesis of several oxygenated derivatives of different types of organic compounds. While free-base porphyrins are useful sensitizers for production of singlet oxygen [5–9], metalloporphyrins are much more versatile photocatalysts due to their coordination ability promoting a wider range of oxidation reactions. They can be applied in autooxidation reactions, hydroxylations or direct oxygen transfer yielding epoxides [10,11]. Cationic manganese(III) porphyrins proved to be efficient catalysts for oxygenation of α-pinene. Its selective epoxidation was observed in aqueous systems at relatively low substrate:catalyst ratio (S/C = 500), while in aprotic organic solvents, such as benzene or toluene, allylic hydroxylation products were formed [12]. Using various metalloporphyrins in acetonitrile, photocatalytic epoxidation of cyclooctene was also achieved [13]. Photocatalytic oxygenation of cycloalkenes [12–14] and other unsaturated heteroaromatics [5] was carried out by application of both metalated and free-base porphyrins [5,12–14].

These precedents inspired us to study the porphyrin-mediated photocatalytic oxygenation of 5,10-methano-5,10-dihydro-4H-benzo[4,5]cyclohepta[1,2-*b*]furan (**1**) (see in Scheme 1) [15]. The structure of this compound represents the basic skeleton of many

---

* Corresponding authors. Tel.: +36 88 624 159; fax: +36 88 624 548 (O. Horváth), tel.: +385 1 4597 241; fax: +385 1 4597 250 (I. Škorić).

E-mail addresses: otto@mk.uni-pannon.hu (O. Horváth), iskoric@fkit.hr (I. Škorić).

0022-2860/$ - see front matter
http://dx.doi.org/10.1016/j.molstruc.2012.09.005

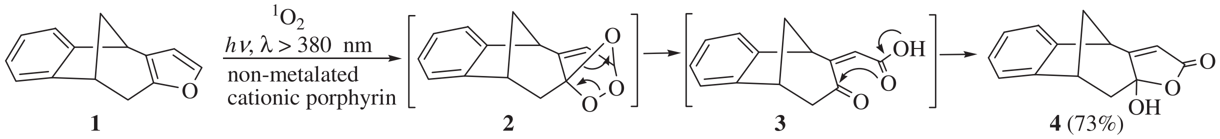

Scheme 1. Simplified mechanism suggested for photocatalytic oxygenation of **1** in the presence of the non-metalated cationic porphyrin (H_2TMPyP^{4+}).

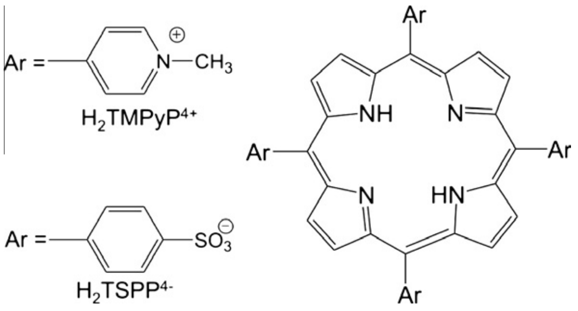

Fig. 1. Structures of 5,10,15,20-tetrakis(1-methyl-4-pyridinium)porphyrin (H_2TMPyP^{4+}) and 5,10,15,20-tetrakis(4-sulfonatophenyl)porphyrin (H_2TSPP^{4-}).

biologically active and important substances isolated from nature, characterized with the same functional groups responsible for their biological activity [16,17].

We have successfully realized the photocatalytic oxygenation of this special benzobicyclodiene containing fused furan ring [15]. The manganese(III) complexes of the cationic 5,10,15,20-tetrakis(1-methyl-4-pyridinium)porphyrin ($Mn(III)TMPyP^{5+}$) and the anionic 5,10,15,20-tetrakis(4-sulfonatophenyl)porphyrin ($Mn(III)TSPP^{3-}$) along with the anionic free base (H_2TSPP^{4-}, Fig. 1) were used in our experiments in aerated and argon-saturated solutions at pH 7. According to our results, in these photocatalytic oxygenation reactions new polycyclic epoxides, enediones, ketones, alcohols and/or hydroperoxides can be obtained, depending on the catalyst applied. The deviating reaction pathways by the different photocatalysts were interpreted in terms of steric and electronic effects.

In order to further elucidate the role of the steric and electronic effects in the photocatalytic oxygenation of this benzobicyclic furan derivative (**1**), we have carried out our experiments at pH 10 too, also using the cationic free base (H_2TMPyP^{5+}, Fig. 1). Additionally, increasing the steric hindrance of the oxidative attack at the outer double bond of the furan ring, photocatalytic oxygenation experiments using both the anionic and the cationic manganese(III) porphyrins and their corresponding free bases were performed with the corresponding benzofuran analogue, 7,12-methano-7,12-dihydro-6H-benzo[4,5]cyclohepta[1,2-*b*]benzo[d]furan (**11**) [18,19] (see in Scheme 3) as an annulated derivative of **1**. Thus, instructive comparisons could be made regarding the structure and the reactivity of both the starting organic substrates and the photocatalysts from the viewpoints of oxygenation. For such analyses reliable structure determination of the products were indispensable. The results of these examinations can serve as useful guiding for planning selective oxygenation of other benzobicyclo[3.2.1]octadiene derivatives in order to get new functionalized bicyclic skeleton found in many natural systems [16].

2. Results and discussion

2.1. Oxygenation of the furan derivative 1

Our previous results regarding the photocatalytic oxygenation of furan derivative **1** have been completed with some experiments using the cationic manganese(III) porphyrin ($Mn(III)TMPyP^{5+}$) and the corresponding free base as catalysts (H_2TMPyP^{4+}). In the presence of the non-metalated cationic porphyrin (in air-saturated solution of pH 7), the product was the same as in the case of the anionic free base (H_2TSPP^{4-}), i.e. hydroxybutenolide derivative **4** as it is shown in Scheme 1.

This phenomenon confirms that application of water-soluble free-base porphyrins, independently of the sign of their charge, results in the formation of the same product because in all cases the oxidative agent in these systems is singlet oxygen. This reactive species is generated by the interaction between dissolved oxygen and long-lived triplet excited state of the porphyrins as sensitizers. The efficiencies for the formation of derivative **4** are very similar (73% for the anionic [15] and 68% for the cationic free base). This phenomenon suggests that in this case the charge of the free-base porphyrins does not significantly influence the yield for the generation of singlet oxygen, in accordance with the interaction of a neutral species, i.e. dioxygen molecule.

In argon-saturated systems no permanent change was observed, confirming that oxygenation with free-base porphyrins as photocatalysts takes place exclusively with a mechanism involving singlet oxygen as the key reactant in situ generated.

As it was previously observed in the case of the anionic manganese(III) porphyrin ($Mn(III)TSPP^{3-}$) [15], an increase of the pH from 7 to 10 significantly enhanced the yield (ratio) of the epoxidized product (**5**) (from 35% to 87%) at the expense of the ring-opened one (**6**) (from 63% to 10%) in air-saturated system [15]. The designations of the compounds are shown in Scheme 2.

This phenomenon suggested that the higher pH hinders the further reaction of derivative **5**. Carried out the experiments with the corresponding cationic metalloporphyrin ($Mn(III)TMPyP^{5+}$), a similar, but much more striking effect was experienced. While at pH 7 (due to electronic effects) the main product in this case was a derivative hydroxylated at an "inner" carbon atom of the furan ring (**9**), at higher pH (=10) the yield of this species considerably diminished (to 8%), and the epoxidized compound (**5**) became the main product with a yield of 74% (Table 1). Notably, this derivative as a product at pH 7 was obtained only in a trace amount (with a yield of 5%).

The striking influence of the increased pH, especially in the case of the cationic manganese(III) porphyrin, may be attributed to the strong reduction of the electrophilicity of the catalyst by a possible axial coordination of a hydroxo ligand. Accordingly, the excited metalloporphyrin is not promoted anymore to attack inner carbon atoms of the furan ring, but formation of the epoxide derivative (**5**) is favorized via oxygenation at the outer double bond, which is sterically much more accessible. Besides, the considerably decreased H^+ concentration might also play a role in the depression of the hydroxylated product (**9**), the formation mechanism of which involves protonation (Scheme 2).

According to earlier works [12] and more recent studies [13,20,21], in the case of manganese(III) porphyrins as photocatalysts, $(P)Mn^{IV}{=}O$ and $(P)Mn^{V}{=}O$ intermediates played the key role of the in situ generated reactive species in the oxygenation of cycloalkenes. $(P)Mn^{IV}{=}O$ can be produced by a photoinduced homolysis of the metal–ligand bond with chloride or hydroxide axial ligands in aqueous systems [11,12]. In the latter case the Mn(II)

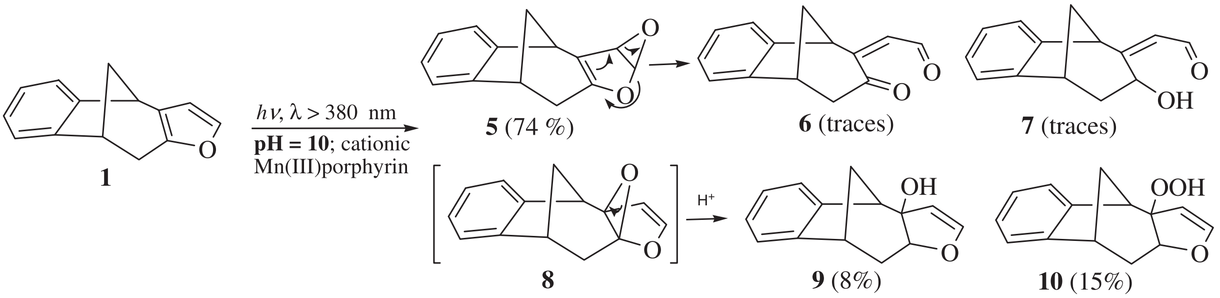

Scheme 2. Simplified mechanisms suggested for photocatalytic oxygenation of **1** in the presence of the cationic manganese(III) porphyrin (Mn(III)TMPyP^{5+}) at pH = 10.

Table 1
Photoproducts with yields (%) obtained using the cationic manganese(III) porphyrin (Mn(III)TMPyP^{5+}) under various experimental conditions.

Compound	9	10	5	6	7
% (pH = 7, air-saturation)	47 [15]	17 [15]	5		
% (pH = 10, air-saturation)[a]	8	15	74	Traces	Traces
% (pH = 7, oxygen-saturation)[a]	13	20	66		

[a] Product ratio in the crude photomixture according to NMR spectra.

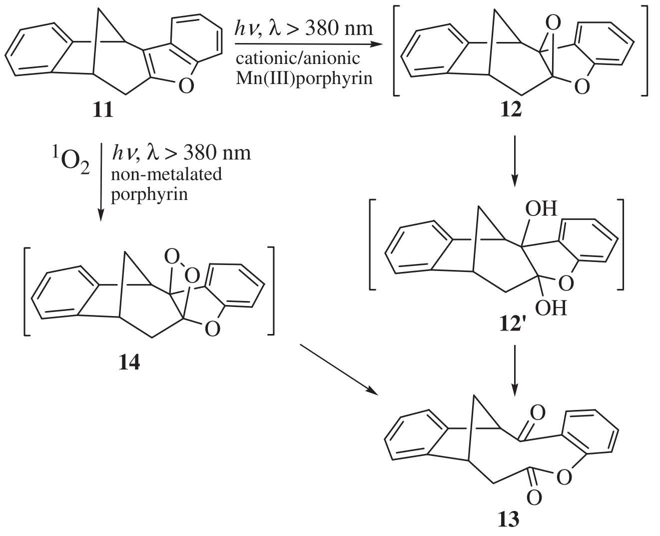

Scheme 3. Simplified mechanisms suggested for photocatalytic oxygenation of **11** in the presence of anionic and cationic manganese(III) porphyrins and the corresponding free bases.

species formed in the primary photochemical step (Eq. (1)) undergoes an oxidation with the dissolved O_2 (Eq. (2)).

$$(\mathrm{P})\mathrm{Mn^{III}OH} + h\nu \rightarrow (\mathrm{P})\mathrm{Mn^{II}} + {}^{\cdot}\mathrm{OH} \tag{1}$$

$$2(\mathrm{P})\mathrm{Mn^{II}} + \mathrm{O_2} \rightarrow 2(\mathrm{P})\mathrm{Mn^{IV}{=}O} \tag{2}$$

Eq. (2) represents an overall reaction comprising several steps [11]. Our experiments were carried out in water–acetone solvent mixture, thus hydroxide or water was axially coordinated to the Mn(III) center. Hence, hydroxyl radicals generated in the primary photochemical step most probably react with the organic solvent. Disproportionation of the Mn(IV) complexes formed produces highly reactive manganese(V)-oxo species (Eq. (3)) [20,21].

$$2(\mathrm{P})\mathrm{Mn^{IV}{=}O} + \mathrm{H^+} \rightleftharpoons (\mathrm{P})\mathrm{Mn^{V}{=}O} + (\mathrm{P})\mathrm{Mn^{III}OH} \tag{3}$$

Disproportionation is significantly faster then synproportionation in this equilibrium system, besides, a polar solvent promotes the previous process, thus it occurs with nearly a diffusion-controlled rate constant [20]. Further, the rate constants for epoxidation of olefins are several orders of magnitude higher for manganese(V)-oxoporphyrins than for the corresponding Mn(IV) species. Accordingly, (P)Mn^{V}=O can be considered as the major oxidant in the photocatalytic oxygenations in our systems.

Also with the manganese(III) porphyrins, experiments were carried out in argon-saturated systems too, at pH 7. Deviating from the corresponding free bases, in the case of which no permanent change was observed due to the exclusive role of the singlet oxygen, the formation of the ring-opened derivative **6** was detected, although with moderate yields, 8% for the anionic and 5% for the cationic metalloporphyrins. This phenomenon suggests that in deoxygenated system the same mechanism of oxygenation is effective, independently of the charge of the porphyrins. The most reasonable way is the photoinduced oxidation of the axially coordinated aqua or (less probably at pH = 7) hydroxo ligands, producing ·OH as shown by Eq. (1). Since a considerable fraction of the hydroxyl radicals formed are scavenged by the organic co-solvent (acetone) in the system, only a minor part of the starting material is transformed to derivative **6** via oxygenation with ·OH.

*2.2. Oxygenation of the benzofuran derivative **11***

In order to study the effect of the increased steric hindrance of the oxidative attack at the outer bond of the furan ring, photocatalytic oxygenation experiments using both the anionic and the cationic manganese(III) porphyrins (Mn(III)TSPP^{3-} and Mn(III)TMPyP^{5+}) and their corresponding free bases (H$_2$TSPP^{4-} and H$_2$TMPyP^{4+}) were carried out with the annulated derivative **11**, which, compared to **1**, contains a benzene connected to the outer side of the furan ring (Scheme 3). Similarly to the case of the furan derivative **1**, the effect of each photocatalyst on the oxygenation of **11** was examined in aerated reaction mixture of pH 7. Besides, changes in the pH and oxygen concentration were also studied with the metalloporphyrin photocatalysts.

Although on the basis of the increased steric hindrance, compared to the products formed from **1**, a much more restricted choice of the oxygenated derivatives of **11** was expected, the results were extreme in this respect. The main product was the same in each case, no matter which catalyst was applied under various conditions. Thus, the photoproduct **13** formed in the presence of the free-base porphyrins agrees with that generated by the use of metalloporphyrins. Structure determination and characterization, based mostly on the results of NMR measurements, unambiguously indicated the formation of the 10-membered keto-lactone derivative **13**, the structure of which is shown in Fig. 2.

The photoproduct **13** (Scheme 3) was isolated by repeated thin-layer chromatography and characterized by spectroscopic methods. From the NMR spectra, using different techniques (COSY, NOESY, HSQC and HMBC), all protons and carbons were assigned due to key interactions (Figs. 3 and 4). The structure of **13** was obvious from the presence of well resolved and well recognizable

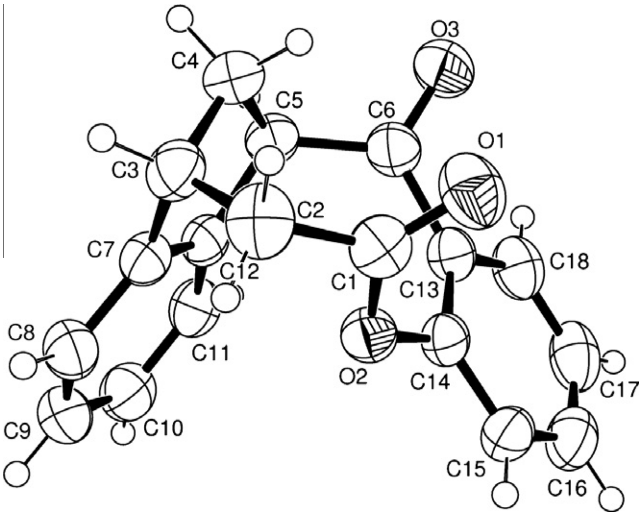

Fig. 2. Molecular structure of **13**. Displacement ellipsoids are drawn for the probability of 50% and hydrogen atoms are depicted as spheres of arbitrary radii.

six-proton-pattern between 2.4 and 4.6 ppm with the characteristic couplings unmistakably pointed to this type of rigid benzobicyclic structures as published earlier [15]. The structure of this photoproduct **13** was confirmed also by its ^{13}C NMR spectrum, which clearly revealed the proposed structure with two characteristic keto groups, two doublets and two triplets in the aliphatic region (see Section 4). There are more complex couplings between the aliphatic protons (Fig. 3), probably due to the changing in the dihedral angles between the C—H bonds of the methano-bridged skeleton in the 10-membered keto-lactone ring, in comparison with the enedione **6** (Scheme 2) obtained from the corresponding furan derivative **1**. Additionally, MS spectra were very informative. Molecular ions *m/z* 278, 32 mass units higher than the starting compound **11**, indicated that two oxygens were added to the molecule of **11**.

The structure and the conformation of **13** were confirmed by single-crystal X-ray diffraction.

Interestingly, this compound formed as the main product in all cases studied is totally different from any type of the product formed from **1** under various experimental conditions. This surprising result suggests that, beside a strong steric hindrance, a considerable electronic effect was also caused by the annulation of a benzene to the outer side of the furan ring.

The same end-product of the application of different photocatalysts does not mean a common oxygenation mechanism. A universal pathway would be in contradiction with the fact that metalloporphyrins can catalyze the oxygenation of **11** even in the absence of dissolved oxygen, while the corresponding free bases cannot be effective in argon-saturated systems, similarly to the case of the furan derivative **1**.

This phenomenon can be attributed to different oxygenation mechanisms leading to the same end-product. The description of the suggested pathways are shown in Scheme 3. In the way for the case of the free bases, similarly to the oxygenation of the furan derivative **1**, singlet oxygen can only be the reactive species generated by the long-lived triplet state of the photocatalysts. However, deviating from the reaction with **1**, the attack at the outer carbon atoms of the furan ring is hindered, and thus, a dioxetane (**14**) formation at the inner double bond is favored, which is followed by a ring fission leading to the end-product **13** [22,23]. In the presence of the metalloporphyrins, as Eqs. (1)–(3) indicate, the reactive species are partly hydroxyl radicals and partly (in aerated systems predominantly) (P)Mn^{IV}=O and (P)Mn^{V}=O molecules. These also attack at the inner carbon atoms of the furan ring, resulting in the formation of an epoxide intermediate **12**, the further reactions of which leads to the final product **13** (Scheme 3). Hydrolysis of epoxide **12** gives an intermediate 1,2-diol **12′**. Either acidic or basic conditions can promote the hydrolysis, giving the intermediate **12′** with *trans* stereochemistry as a result of the stereospecificity of the reaction. The 10-membered keto-lactone end-product **13** is formed by further oxidative cleavage of the cyclic 1,2-diol **12′** to the corresponding dicarbonyl compound in a way similar to that described for the oxidative cleavage of some β-hydroxyethers [24,25].

In comparison with the 10-membered keto-lactone end-product **13**, intermediates **12** and **12′** are also very interesting for their different rigid methano-bridged junction of two aromatic units at defined geometrical arrangement (Fig. 5), and the changes in the structure according to the space filling models can be followed for the reaction of conversion from the starting substrate **11** into **13**.

In the case of the free-base porphyrins the yields of the end-product **13** are high, approaching the total conversion (99% for H_2TSPP^{4-} and 85% for H_2TMPyP^{4+} at pH 7 in aerated solution) so this reaction can be characterized as a very efficient entry into medium-ring keto-lactones. This data indicate that the formation of singlet oxygen is very efficient for both free bases. Like in the case of the furan derivative **1**, the similar yields confirm that the charge of the sensitizer does not play any role in the interaction with the neutral dioxygen molecule. Besides, the absorption

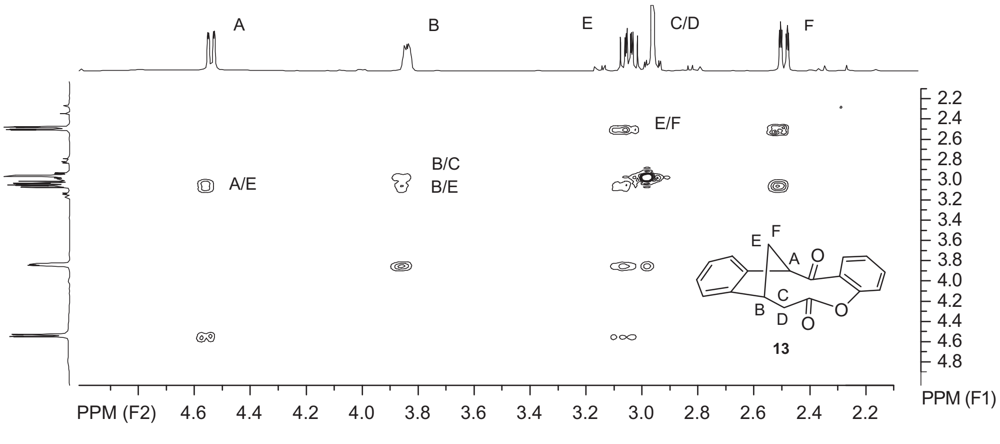

Fig. 3. COSY spectrum of the keto-lactone end-product **13** in $CDCl_3$ (600 MHz).

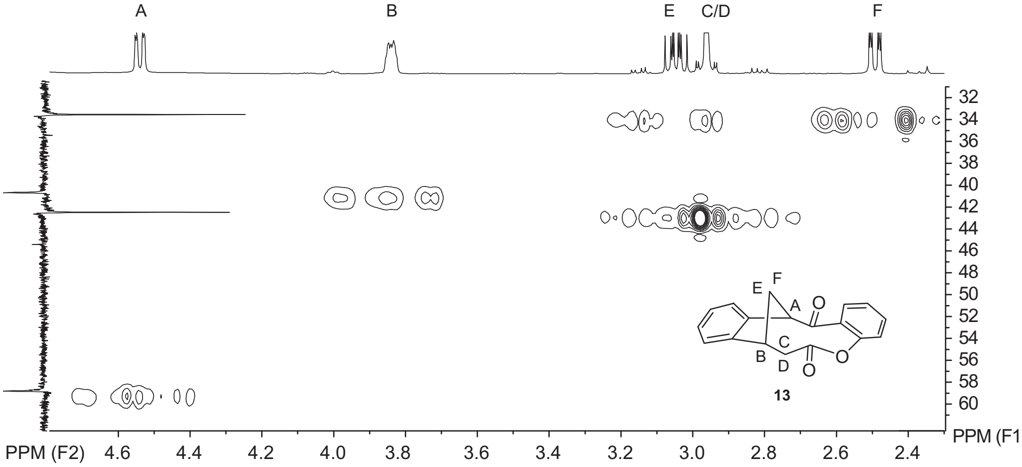

Fig. 4. HSQC spectrum of the keto-lactone end-product **13** in $CDCl_3$ (600 MHz).

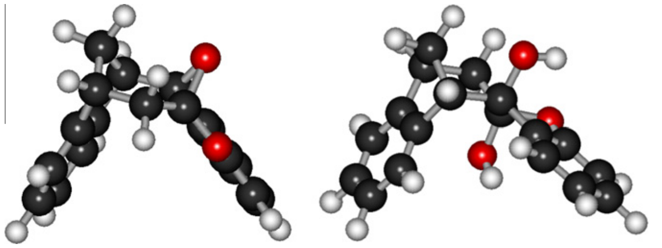

Fig. 5. Space filling models of the reaction intermediates **12** (left) and **12′** (right) during the reaction according to Scheme 3.

Table 2
The yields (%) of the photoproduct **13** obtained by using anionic and cationic manganese(III) porphyrins under various experimental conditions.

	Mn(III)TSPP^{3-}	Mn(III)TMPyP^{5+}
% (pH = 7, air saturation)	40	81
% (pH = 10, air saturation)	36	83
% (pH = 7, oxygen saturation)	13	85
% (pH = 7, argon saturation)	11	14

spectra of these porphyrins and the lifetimes of their triplet states are also very similar [26,27].

The yields of the common end-product obtained with the manganese(III) porphyrins applied at various circumstances are summarized in Table 2.

Deviating from the results with the free bases, the photocatalytic oxygenation efficiency of the corresponding manganese(III) porphyrins strongly depends on the their charge. The yields for the cationic catalyst are over 80% under each condition applied, while those for the anionic one do not exceed 40%. The significantly higher efficiencies for Mn(III)TMPyP^{5+} can be attributed to the lower Lewis basicity of the porphyrin ligand making the corresponding manganese(V)-oxo intermediate much more electrophilic than the anionic one.

An increase of the pH from 7 to 10 did not cause any significant change in the yields of the end-product (a slight decrease for the anionic and an even slighter increase for the cationic metalloporphyrins, Table 2). This phenomenon suggests that protons (or hydroxide ions) are not involved in rate-determining steps of this mechanism. Increasing the concentration of dissolved O_2 (using oxygen-saturated system), no appreciable change was observed for the cationic photocatalyst, while a dramatic reduction of the yield (to about one third of that obtained in aerated solution) occurred for Mn(III)TSPP^{3-}. These deviating results may be attributed to a quenching effect of the oxygen, decreasing the efficiency of the primary photochemical step (Eq. (1)). Thus, a decrease in the concentration of the less electrophilic anionic Mn(V)-oxo intermediate significantly diminishes the oxygenation yield, while in the case of the corresponding cationic species, which is a much more effective reagent, such a reduction of the concentration does not influence the yield of the end-product.

In the case of argon-saturated systems, similarly to the results with the furan derivative **1**, dramatic reductions of the yield for both manganese(III) porphyrins were observed. The values of the yield are very similar, independently of the charge of the catalyst, confirming, as suggested for the case of **1**, that the hydroxyl radicals formed in the primary photochemical step (Eq. (1)) are the common oxidative agents. A significant part of these species are scavenged by the organic co-solvent, strongly diminishing the efficiency of the oxygenation of **11**. The moderately lower yield with the anionic catalyst is in accordance with its higher Lewis basicity decreasing the efficiency of the photoinduced LMCT reaction generating $^{\cdot}OH$ from the axially coordinated aqua (or hydroxo) ligand. Notably, also in the case of the furan derivative **1**, the end-product in argon-saturated systems was the corresponding ring-opened compound (**6**).

3. Conclusions

The comparison of the photocatalytic oxygenation of a furan derivative of the benzobicyclo[3.2.1]octadiene skeleton **1** and that of the corresponding benzofuran derivative **11** revealed striking differences. In the previous case, the application of free-base porphyrins led to the formation of a hydroxybutenolide derivative, and the use of cationic and anionic manganese(III) porphyrins generated various other oxygenated products such as epoxidized and furan ring-opened compounds (with the Mn(III)TSPP^{3-} catalyst) as well as hydroperoxy- and hydroxy-derivatives (with Mn(III)TMPyP^{5+}). An increase of pH, diminishing the electrophilicity of the cationic metalloporphyrin, promoted the reaction producing the epoxidized product. However, photocatalytic oxygenation of the benzofuran derivative **11** resulted in the formation of only one end-product, independently of the photocatalyst applied. This phenomenon indicated that, although the free bases and the corresponding manganese(III) porphyrins catalyze the oxygenation via different mechanisms, generating singlet oxygen and Mn(V) or $^{\cdot}OH$ species as reactive oxidants, respectively, the

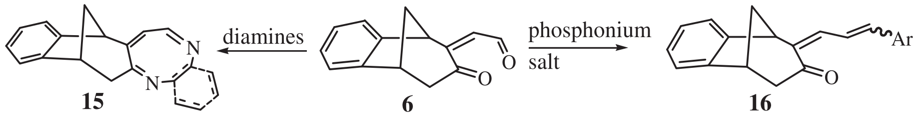

Scheme 4. Further possible applications of the photocatalytic oxygenation by manganese(III) porphyrins.

strong electronic and steric effects allow the formation of only one type of compound, the bridged 10-membered keto-lactone **13**. These results demonstrate that annulation of a benzene to the outer side of the furan ring dramatically restricts the possibilities of this photocatalytic oxygenation giving a very interesting 10-membered keto-lactone structure, which was found in many natural compounds too [28,29]. On this way, the applied benzofuran derivative **11** proved to be excellent selective precursor of the medium-sized macrolactone ring **13**. Accordingly, the type of the end-product can be controlled by the porphyrin catalyst (anionic, cationic, metalated or free-base), the pH, and the structural modification of the basic skeleton.

Utilization of this type of photocatalytic oxygenation can also be applied for synthesis of other novel benzobicyclo[3.2.1]octadiene derivatives with nitrogen (**15**), even more similar to natural structures, by their subsequent transformations with different diamines to water-soluble derivatives or rigid-methano-bridged skeleton with prolonged double bond (**16**) as shown in Scheme 4.

Water-soluble free-base and metalloporphyrins as catalysts for oxygenation of organic substrates in water–acetone solvent mixture offer the possibility of their easy separation from the products, ensuring the efficient reuse of them. This peculiarity may be a considerable advantage over the fully hydrophobic systems.

4. Experimental section

4.1. General

The ^{1}H and ^{13}C NMR spectra were recorded in $CDCl_3$ solutions containing tetramethylsilane as internal standard on a Bruker Spectrometer at 300 or 600 and at 75 or 150 MHz, respectively. The mass spectra were recorded on a GC/MS instrument (GC temperature program: delay 3 min, injector temperature 350 °C, heating from 110 to 300 °C within 6 min, then 300 °C isothermal for 15 min). Elemental analysis was carried out on Perkin–Elmer, Series II, CHNS Analyzer 2400. Chromatographic separations were performed on thin layer plates (0.2 mm, Kiselgel 60 F_{254}, Merck). All solvents were distilled prior the use.

4.2. Typical experimental procedure for the photocatalytic oxygenation of **1** and **11**

A solution of 40 ml of **1** or **11** and the manganese(III) and free-base porphyrins in acetone/water (50:50) was irradiated with a 70 W tungsten halogen immersion lamp (Philips, $\lambda_{ir} > 380$ nm) in a thermostated 50 ml cylindrical photoreactor. A stream of air or oxygen was passed through the solution at RT during 2 h, also ensuring vigorous stirring. The following concentrations conditions were: S/C = 100, porphyrin = 0.00144 mmol and **1** or **11** = 0.144 mmol. After termination of the photolysis acetone was removed by vacuum distillation. The remaining two phases were separated by standard methods. The water-insoluble oxygenation products remained in the organic phase. The photoproducts **4**, **5**, **9** and **10** from **1** and **13** from **11** (Schemes 1–3), were isolated by repeated thin-layer chromatography using petroleum ether/diethyl ether (20–50%) as eluent and characterized by spectroscopic methods.

Table 3
Crystallographic data collection and structure refinement details.

Compound	13
Empirical formula	$C_{18}H_{14}O_3$
Formula wt./g mol^{-1}	278.29
Crystal dimensions/mm	0.37 × 0.28 × 0.18
Space group	$P\bar{1}$
a (Å)	7.2175(5)
b (Å)	9.4768(8)
c (Å)	10.1521(8)
α (°)	77.261(7)
β (°)	84.498(6)
γ (°)	87.794(6)
Z	2
V (Å^3)	674.07(9)
D_{calc} (g cm^{-3})	1.371
μ (mm^{-1})	0.753
Θ range (°)	4.48–75.95
T (K)	293(2)
Diffractometer type	Xcalibur Nova
Range of h, k, l	$-7 < h < 9$ $-11 < k < 11$ $-10 < l < 12$
Reflections collected	4840
Independent reflections	2645
Observed reflections ($I \geqslant 2\sigma$)	2217
Absorption correction	Multi-scan
R_{int}	0.0343
R (F)	0.0495
R_w (F^2)	0.1511
Goodness of fit	1.073
H atom treatment	Constrained
No. of parameters	191
$\Delta\rho_{max}, \Delta\rho_{min}$ (e Å^{-3})	0.228; −0.243

4.3. 8,13-methano-8,13-dihydrodibenz[b,f]oxecane-6(7H),14-dione (13)

Colorless oil; UV (96% ethanol): λ_{max} (ε) 244 nm (6707 mol^{-1} dm^3 cm^{-1}); IR (ν_{max}, cm^{-1}, evaporated from diethylether): 1762 and 1650 (C=O).^{1}H NMR (600 MHz, $CDCl_3$): δ_H 2.49 (1H, m, H_F), 2.96 (2H, m, $H_{C/D}$), 3.05 (1H, m, H_E), 3.4 (1H, m, H_B), 4.54 (1H, dd, J = 4.5; 2.9 Hz, H_A), 6.91 (1H, d, J = 7.6 Hz, H_{ar}), 7.03 (1H, t, J = 7.4 Hz, H_{ar}), 7.19 (1H, m, H_{ar}), 7.20 (1H, t, J = 7.4 Hz, H_{ar}), 7.22 (1H, dt, J = 7.6; 0.9 Hz, H_{ar}), 7.28 (1H, d, J = 7.6 Hz, H_{ar}), 7,37 (1H, ddt, J = 7.8; 1.7; 0.6 Hz, H_{ar}), 7.72 (1H, dd, J = 7.8; 1.7 Hz, H_{ar}). ^{13}C NMR (150 MHz, $CDCl_3$) δ_C33.5 (t), 40.6 (d), 42.5 (t), 58.8 (d), 121.3 (d), 124.0 (d), 124.9 (d), 125.3 (d), 127.1 (d), 127.5 (d), 129.9 (s), 130.2 (d), 132.1 (d), 139.8 (s), 145.6 (s), 147.5 (s), 167.8 (s), 203.6 (s). MS, m/z (%) = 278 (M$^+$, 100). Anal. Calcd for $C_{18}H_{14}O_3$: C, 77.68; H, 5.07. Found: C, 77.45; H 5.29.

4.4. Single-crystal X-ray structure analysis of **13**

Single crystal measurement was performed on an Oxford Diffraction Xcalibur Nova R (CCD detector, microfocus Cu tube). Program package CrysAlis PRO [30] was used for data reduction. The structures were solved using SHELXS97 [31] and refined with SHELXL97 [31]. The model was refined using the full-matrix least squares refinement; all non-hydrogen atoms were refined anisotropically. Hydrogen atoms were treated as riding entities. Drawing of the molecular structure was prepared using ORTEP-3 [32].

Crystallographic and refinement data for the structures reported in this paper are shown in Table 3.

Supplementary material

Supplementary crystallographic data for this paper can be obtained free of charge via www.ccdc.cam.ac.uk/conts/retrieving.html (or from the Cambridge Crystallographic Data Centre, 12, Union Road, Cambridge CB2 1EZ, UK; fax:+44 1223 336033; or deposit@ccdc.cam.ac.uk). CCDC 871751 contains the supplementary crystallographic data for this paper.

Acknowledgements

This research was funded by a grant from the Ministry of Science, Education and Sports of the Republic of Croatia (125-0982933-2926). It has been realized also with the support of the Hungarian Government and the European Union, with the co-funding of the European Social Fund in the frame of the projects TÁMOP-4.2.1/B-09/1/KONV-2010-0003 and TÁMOP-4.2.2/B-10/1-2010-0025. We would also like to thank Dr. Krešimir Molčanov for the single-crystal X-ray structural analysis of **13**.

References

[1] L.R. Milgrom, The Colours of Life: An Introduction to the Chemistry of Porphyrins and Related Compounds, Oxford University Press, Oxford, 1997. p. 15–18 and 101–115.

[2] O.T. Woo, W.K. Chung, K.H. Wong, A.T. Chow, P.K. Wong, J. Hazard. Mater. 168 (2009) 1192.

[3] E. Szabó-Bárdos, O. Markovics, O. Horváth, N. Törő, G. Kiss, Water Res. 45 (2011) 1617.

[4] S. Weimin, Z. Gen, D. Guifu, Z. Yunxiao, Z. Jin, T. Jingchao, Med. Chem. 16 (2008) 5665.

[5] K. Gollnick, A. Griesbeck, Tetrahedron 41 (1985) 2057.

[6] N.J. Turro, Modern Molecular Photochemistry, University Science Books, Sausalito, 1991. p. 587–593.

[7] M.R. Iesce, F. Cermola, A. Guitto, R. Scarpati, M.L. Graziano, J. Org. Chem. 60 (1995) 5324.

[8] C.J.P. Monteiro, M.M. Pereira, M.E. Azenha, H.D. Burrows, C. Serpa, L.G. Arnaut, M.J. Tapia, M. Sarakha, P. Wong-Wah-Chung, S. Navaratnam, Photochem. Photobiol. Sci. 4 (2005) 617.

[9] T. Montagnon, M. Tofi, G. Vissilikogiannakis, Acc. Chem. Res. 41 (2008) 1001.

[10] L. Weber, R. Hommel, G. Haufe, J. Behling, H. Hennig, J. Am. Chem. Soc. 116 (1994) 2400.

[11] H. Hennig, J. Behling, R. Meusinger, L. Weber, Chem. Ber. 128 (1995) 229.

[12] H. Hennig, Coord. Chem. Rev. 182 (1999) 101 (and references therein).

[13] M. Hajimohammadi, F. Bahadoran, S.S.H. Davarani, N. Safari, React. Kinet. Mech. Cat. 99 (2010) 243.

[14] A. Maldotti, L. Andreotti, A. Molinari, G. Varani, G. Cerichelli, M. Chiarini, Green Chem. 3 (2001) 42.

[15] I. Kikaš, O. Horváth, I. Škorić, Tetrahedron Lett. 52 (2011) 6255.

[16] D.C. Ericsson, L.E. Cuca, M. Sefkow, J. Nat. Prod. 72 (2009) 1245.

[17] K. Yoganathan, S. Cao, S.C. Crasta, S. Aitipamula, S.R. Whitton, S. Ng, A.D. Buss, M.S. Butler, Tetrahedron 64 (2008) 10181.

[18] M. Šindler-Kulyk, I. Škorić, S. Tomšić, Ž. Marinić, D. Mrvoš-Sermek, Heterocycles 51 (1999) 1355.

[19] I. Škorić, N. Basarić, Ž. Marinić, M. Šindler-Kulyk, Heterocycles 55 (2001) 1889.

[20] R. Zhang, J.H. Horner, M. Newcomb, J. Am. Chem. Soc. 127 (2005) 6573.

[21] M. Newcomb, R. Zang, Z. Pan, D.N. Harischandra, R.E.P. Chandrasena, J.H. Horner, E. Martinez, Catal. Today 117 (2006) 98.

[22] H.H. Wasserman, A.R. Doumaux, J. Am. Chem. Soc. 84 (1962) 4611.

[23] A.P. Schaap, K.A. Zaklika, B. Kaskar, L.W.M. Fung, J. Am. Chem. Soc. 102 (1980) 389.

[24] H.M.C. Ferrazand, L.S. Longo Jr., J. Org. Chem. 72 (2007) 2945.

[25] H.M.C. Ferraz, L.S. Longo Jr., Org. Lett. 5 (2003) 1337.

[26] P.D. Harvey, in: K.M. Kadish, K.M. Smith, R. Guilard (Eds.), The Porphyrin Handbook, 18, Academic Press, San Diego, 2003, pp. 63–250.

[27] R. Dědic, V. Vyklický, A. Svoboda, J. Hála, J. Mol. Struct. 924–926 (2009) 153.

[28] A. Parenty, X. Moreau, J.-M. Campagne, Chem. Rev. 106 (2006) 911.

[29] R.A. Edrada, M. Heubes, G. Brauers, V. Wray, A. Berg, U. Gräfe, M. Wohlfarth, J. Mühlbacher, K. Schaumann, J. Nat. Prod. 65 (2002) 1598.

[30] CrysAlis PRO, Oxford Diffraction Ltd., UK, 2007.

[31] G.M. Sheldrick, Acta Crystallogr. A A64 (2008) 112.

[32] L.J. Farrugia, J. Appl. Cryst. 30 (1997) 565.